Electron collisions with $BF^+$: bound and continuum states of BF



2011 J. Phys. B: At. Mol. Opt. Phys. 44 055203

(http://iopscience.iop.org/0953-4075/44/5/055203)

J. Phys. B: At. Mol. Opt. Phys. **44** (2011) 055203 (8pp) doi:10.1088/0953-4075/44/5/055203

# Electron collisions with $BF^+$: bound and continuum states of BF

**K Chakrabarti[1,2], I F Schneider[2,3] and Jonathan Tennyson[4]**

[1] Department of Mathematics, Scottish Church College, 1 & 3 Urquhart Sq., Kolkata 700006, India
[2] Laboratoire Ondes et Milieux Complexes (LOMC) CNRS-FRE-3102, Université du Havre, 25, rue Philippe Lebon, BP 540, 76058 Le Havre, France
[3] Laboratoire Aimeé Cotton, CNRS-UPR-3321, Université Paris-Sud, Bâtiment 505, 91405 Orsay, France
[4] Department of Physics and Astronomy, University College London, Gower St., London WC1E 6BT, UK

E-mail: j.tennyson@ucl.ac.uk

Received 30 November 2010, in final form 11 January 2011
Published 7 February 2011
Online at stacks.iop.org/JPhysB/44/055203

**Abstract**
Rydberg and continuum states of the BF molecule are studied as a function of geometry using an electron collision formalism in the framework of the *R*-matrix method. Up to 14 $BF^+$ target states are used in a close-coupling expansion and bound states are searched for as negative energy solutions of the scattering calculation. Potential energy curves and quantum defects are obtained for the excited states of BF. Resonance positions and widths are also calculated for Feshbach resonances in the system. The data obtained can be used to model dissociative recombination of the $BF^+$ molecular ion.

(Some figures in this article are in colour only in the electronic version)

## 1. Introduction

Electron collisions with the $BF^+$ ion occur in $BF_3$ plasmas, which play an important role in ion doping of silicon wafers. In such environments, low energy electron collisions can result in excitation, de-excitation and destruction of molecular ions. The principal route for the latter process is dissociative recombination (DR). DR studies, particularly those based on multichannel quantum defect theory (MQDT) (see, for example, Giusti (1980), Schneider *et al* (2000)), require knowledge of the neutral dissociative states (in this case those of the BF molecule), and of their coupling with the ionization continua. The *R*-matrix formalism allows their determination from electron scattering calculation on $BF^+$. It is one of the aims of this paper to provide these data.

Considerable literature exists on the BF molecule which, like CO, is a 14-electron system. Properties of the $^1\Sigma^+$ ground state of BF were studied by Kurtz and Jordan (1981). Rosmus *et al* (1982) also studied the ground state of BF along with the ground state of $BF^+$ over a wide range of internuclear distances. Schneider and Gianturco (1988) obtained potential energy curves for the ground state and the $A^1\Pi$ excited state. Other works on BF are due to Bredohl *et al* (1988), da Costa *et al* (1992), Honingmann *et al* (1993), Mérawa *et al* (1997). In particular, Honingmann *et al* (1993) and Mérawa *et al* (1997) provided potential energy curves for several excited singlet and triplet states.

In this paper we provide positions and widths for Feshbach resonances in the e–$BF^+$ system. In addition we also study the bound states of this system which results in potential energy curves and quantum defects of the ground and Rydberg states of the BF molecule. The data we obtain can be used as a starting point for the calculation of DR of the $BF^+$ ion.

## 2. Calculations

### 2.1. Method

Details of the calculation can be found in our earlier work (Chakrabarti and Tennyson 2009) and only the essential parts are presented. The *R*-matrix method divides the configuration space into two regions (Burke and Berrington 1993), an inner region defined by a sphere, here of radius 10 $a_0$, centred at the molecular centre of mass. This sphere encloses the entire *N*-electron target $BF^+$ wavefunction. In this inner region, the wavefunction of the $(N+1)$-electron system ($BF^+$ + electron)

 

is given by

$$\Psi_k = \mathcal{A}\sum_{i,j} a_{i,j,k}\Phi_i(1,\ldots,N)F_{i,j}(N+1) + \sum_i b_{i,k}\chi_i(1,\ldots,N+1), \quad (1)$$

where $\mathcal{A}$ is the antisymmetrization operator, $F_{i,j}$ are the continuum orbitals and $\chi_i$ are the two-centre $L^2$ functions constructed from $N$-electron target orbitals. Here $\Phi_i$ is the wavefunction of the $i$th target state. Electron-correlation effects are included in these target wavefunctions via configuration interaction (CI) expansions and the variational coefficients $a_{i,j,k}$ and $b_{i,k}$ are determined by diagonalizing the Hamiltonian matrix. Note that the $L^2$ functions are important for incorporating correlation–polarization effects in the calculation; this is discussed extensively in previous $R$-matrix studies, see Tennyson (1996b) for example.

We used the diatomic version of the UK molecular $R$-matrix codes (Morgan *et al* 1998) which uses Slater-type orbitals (STOs). The target and numerical orbitals used to represent the continuum (Tennyson and Morgan 1999) rely on STOs. A Buttle (1967) correction was used to allow for the arbitrary fixed boundary conditions imposed on the continuum basis orbitals. For an overview of the whole procedure see the recent review by Tennyson (2010).

### 2.2. The $BF^+$ target

Calculation on both $BF^+$ and BF was performed at 11 internuclear separations in the range 1.5–3.5 $a_0$. The VB2 STOs of Ema *et al* (2003) were used to build a molecular basis of 46 molecular orbitals ($24\sigma$, $14\pi$, $6\delta$, $2\phi$). An initial SCF calculation was performed using these molecular orbitals for the lowest $^2\Sigma^+$ and $^2\Pi$ states of $BF^+$. The SCF molecular orbitals were then used in a CI calculation. In all cases $1\sigma$ and $2\sigma$ orbitals were frozen and the CI calculations were performed using the configurations

$(3\sigma, 4\sigma, 5\sigma, 1\pi)^9$,
$(3\sigma, 4\sigma, 5\sigma, 1\pi)^8$ $(6\sigma$–$24\sigma, 2\pi$–$14\pi, 1\delta$–$6\delta)^1$,
$(3\sigma, 4\sigma, 5\sigma, 1\pi)^7$, $(6\sigma$–$24\sigma, 2\pi$–$14\pi, 1\delta$–$6\delta)^2$,

which correspond respectively to the complete active space (CAS) spanning valence orbitals, CAS plus single excitations out of the CAS and CAS plus double excitations.

Two sets of pseudo natural orbitals (NOs) were initially obtained by CI calculation on the lowest $^2\Sigma^+$ and $^2\Pi$ states of $BF^+$. In the subsequent target state calculation, all $\sigma$ orbitals and one $\pi$ orbital in the target wavefunction were represented by $^2\Sigma^+$ NOs and the remaining $\pi$ orbitals and all $\delta$ orbitals were represented by $^2\Pi$ NOs.

Our target model uses the NOs as above and a $(3\sigma, 4\sigma, 5\sigma, 6\sigma, 1\pi, 2\pi)^9$ CAS-CI wavefunction. The vertical excitation energies at the BF equilibrium bond length 2.386 $a_0$, potential energy curves and dipole moments were obtained in our earlier work (Chakrabarti and Tennyson 2009) and were in good agreement with other relevant data.

**Table 1.** Quantum defects and vertical excitation energies (in eV) from the $X^1\Sigma^+$ ground state of the BF molecule at $R_e = 2.386\ a_0$. The quantum defects for the experiments and other theories presented could not be provided since the corresponding ionization potentials were not known.

| Excited state | This work | | Experiment[a] | MRD-CI[b] | TDGI[c] |
|---|---|---|---|---|---|
| $B^1\Sigma^+$ $3s\sigma$ | 0.887 | 8.14 | 8.10 | 7.98 | 8.04 |
| $C^1\Sigma^+$ $3p\sigma$ | 0.639 | 8.54 | 8.55 | 8.38 | 8.51 |
| $G^1\Sigma^+$ $3d\sigma$ | 0.0007 | 9.46 | 9.54 | | 9.58 |
| $H^1\Sigma^+$ $4s\sigma$ | 0.782 | 9.66 | 9.84 | | 9.67 |
| $I^1\Sigma^+$ $4p\sigma$ | 0.619 | 9.79 | 9.87 | | 9.95 |
| $L^1\Sigma^+$ $5s\sigma$ | 0.774 | 10.22 | 10.33 | | |
| $O^1\Sigma^+$ $5p\sigma$ | 0.614 | 10.27 | 10.37 | | |
| $R^1\Sigma^+$ $6s\sigma$ | 0.770 | 10.48 | 10.64 | | |
| $^1\Pi$ | | | | | |
| $A^1\Pi$ $2p\pi$ | 0.166 | 6.93 | 6.34 | 6.56 | 6.33 |
| $D^1\Pi$ $3p\pi$ | 0.388 | 8.98 | 8.94 | | 8.87 |
| $F^1\Pi$ $3d\pi$ | −0.042 | 9.51 | 9.59 | | 9.72 |
| $J^1\Pi$ $4p\pi$ | 0.421 | 9.91 | 9.98 | | 9.92 |
| $P^1\Pi$ $5p\pi$ | 0.431 | 10.33 | 10.42 | | |
| $^1\Delta$ | | | | | |
| $E^1\Delta$ $3d\delta$ | 0.057 | 9.41 | 9.45 | | |
| $^3\Sigma^+$ | | | | | |
| $b^3\Sigma^+$ $3s\sigma$ | 0.983 | 7.63 | 7.56 | 7.52 | |
| $c^3\Sigma^+$ $3p\sigma$ | 0.727 | 8.34 | 8.31 | 8.2 | |
| $e^3\Sigma^+$ $3d\sigma$ | 0.104 | 9.36 | 9.41 | | |
| $g^3\Sigma^+$ $4s\sigma$ | 0.703 | 9.73 | 9.76 | | |
| $^3\Pi$ | | | | | |
| $a^3\Pi$ $2p\pi$ | 0.621 | 3.83 | 3.61 | 3.57 | |
| $d^3\Pi$ $3p\pi$ | 0.542 | 8.73 | 8.76 | | |
| $f^3\Pi$ $3d\pi$ | −0.042 | 9.51 | 9.59 | | |
| $h^3\Pi$ $4p\pi$ | 0.522 | 9.85 | 9.94 | | |

[a] Experiment from Huber and Herzberg (1979), also available from the NIST chemistry webbook (http://webbook.nist.gov/chemistry/).
[b] Honingmann *et al* (1993). [c]Mérawa *et al* (1997).

### 2.3. The BF model

Our calculations use 14 $(8\sigma, 4\pi, 2\delta)$ $BF^+$ NOs. They were augmented by continuum orbitals $F_{i,j}$, expressed as truncated partial waves around the centre of mass. Partial waves with $l \leqslant 6$ and $m \leqslant 2$ were retained in the expansion. Convergence in this partial wave expansion was checked with respect to the bound state energies, resonance positions and widths. We took $l \leqslant 6$ because inclusion of higher partial waves did not give any significant difference in these quantities. The radial parts of the continuum functions were generated as numerical solutions of an isotropic Coulomb potential. Those solutions with an energy below 10 Ryd were retained. A Buttle (1967) correction was used to compensate the effect of this truncation or, alternatively, the fixed boundary condition used to generate the functions. To correct for linear dependence effects, four $\sigma$ orbitals were removed using Lagrange orthogonalization (Tennyson *et al* 1987). The resulting 153 ($59\sigma$, $52\pi$, $42\delta$) functions were Schmidt orthogonalized to the target NOs.

Calculations were performed using the $(3\sigma$–$6\sigma, 1\pi, 2\pi)^9$ CAS target wavefunction for the $BF^+$ states. Target orbitals not used in the CAS were treated in the same fashion as the continuum functions, $F_{i,j}$ in equation (1), and contracted with

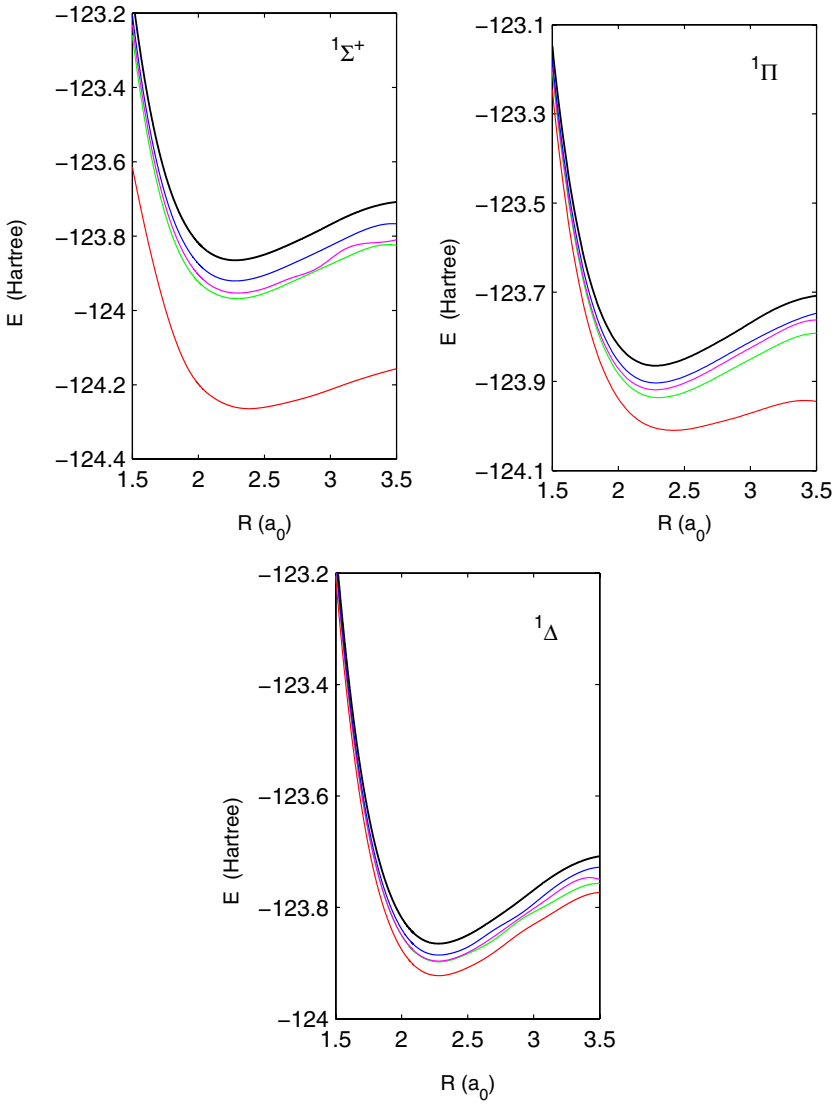


**Figure 1.** Potential energy curves of the lowest four states of the BF molecule for the symmetries $^1\Sigma^+$, $^1\Pi$ and $^1\Delta$. The topmost curve in black in each figure is the $BF^+$ $X^2\Sigma^+$ ground state.

the target CI (Tennyson 1996a). All calculations used an *R*-matrix radius of 10 $a_0$ except those performed for BF bond lengths $R = 3.1, 3.3$ and $3.5\,a_0$ for which the *R*-matrix radius was chosen to be $12\,a_0$ to accommodate a larger target size.

Calculations were performed for the states of both singlet and triplet symmetries so that the bound states and resonances we consider are of total symmetry $^1\Sigma^+$, $^1\Pi$, $^1\Delta$, $^3\Sigma^+$, $^3\Pi$ and $^3\Delta$.

### 2.4. Bound states

The inner region solutions thus obtained are used to construct an *R*-matrix on the boundary. In the outer region, in addition to the Coulomb potential, the potential was given by the diagonal and off-diagonal dipole and quadrupole moments of the $BF^+$ target states. To find bound states, asymptotic outer region wavefunctions were constructed using a Gailitis expansion (Noble and Nesbet 1984) and then integrated inwards to the *R*-matrix boundary. For this work *R*-matrices were propagated to 50 $a_0$ and an improved Runge–Kutta–Nystrom procedure implemented by Zhang *et al* (2011) was used.

Bound states were then found using the searching algorithm of Sarpal *et al* (1991) with the improved nonlinear, quantum defect-based grid of Rabadán and Tennyson (1996). Not all target states included in the inner region close-coupling expansion were explicitly treated in the outer region, as the inclusion of these states was found to make little numerical difference.

### 2.5. Resonances

For the resonance calculation, *R*-matrices were propagated (Morgan 1984) to 100 $a_0$, as tests showed that this produced stable results, and then matched with a Gailitis expansion (Noble and Nesbet 1984). Details of the procedure can also be found in our earlier work (Chakrabarti and Tennyson 2009) where resonance positions and widths were presented at the equilibrium geometry.

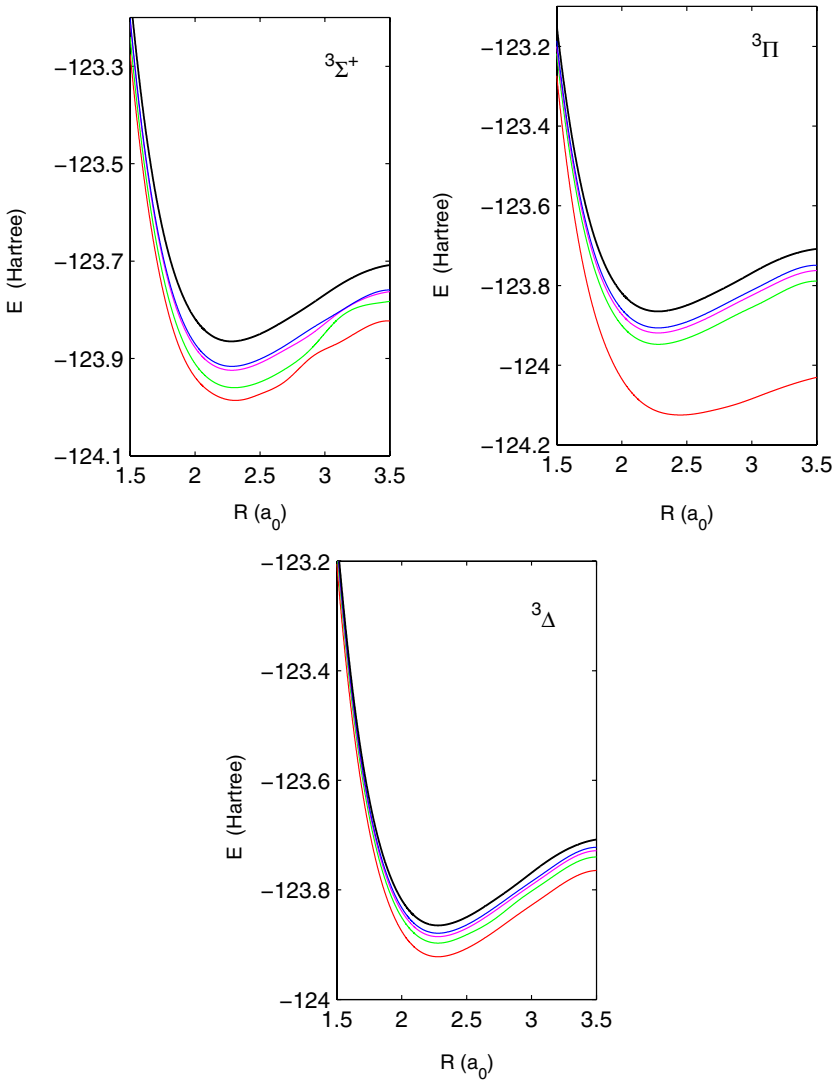


**Figure 2.** Potential energy curves of the lowest four states of the BF molecule for the symmetries $^3\Sigma^+$, $^3\Pi$ and $^3\Delta$. The topmost curve in black in each figure is the $BF^+$ $X^2\Sigma^+$ ground state.

Resonances were detected and fitted to a Breit–Wigner profile to obtain their energy ($E$) and width ($\Gamma$) using the RESON program (Tennyson and Noble 1984) with an energy grid $0.25\times10^{-3}$ Ryd. The magnitudes of the complex quantum defects $\mu = \alpha + i\beta$ were obtained using the relations

$$E_r = E_t - \frac{1}{\nu^2}, \qquad \Gamma = \frac{2\beta}{\nu^3} \tag{2}$$

where the effective quantum number $\nu$ equals $n - \alpha$ and $E_t$ is the energy of the threshold to which the Rydberg series converges.

## 3. Results

### *3.1. Rydberg states at equilibrium bond length*

In table 1 we compare the vertical excitation energies for some of the excited states of BF with experiments and other calculations. Our calculated excitation energies are in good agreement with the experiments and other theories. Except for the $A^1\Pi$ state, all the other excitation energies are within 0.2 eV of the experiments and also of the MRD-CI and TDGI calculations. We also present our quantum defects for these states; however, quantum defects for the experiments and the MRD-CI and TDGI calculations are unavailable.

An important parameter for the quality of the calculation is the ionization potential (IP) of the system, which is often ignored in many *ab inito* calculations. The IP of BF determined by Dyke *et al* (1983) using high temperature photoelectron spectroscopy was quoted to be 11.12 ± 0.01 eV. They found the vertical and adiabatic IPs to be coincident. This compared well with the value 11.06±0.10 eV, which was found earlier by Hildenbrand (1971) using electron impact mass spectrometry. On the theoretical side, calculations of Schneider and Giunturco (1988) gave a vertical IP of 9.9 eV at the SCF level and 10.9 eV by the CI calculation which was close to the MCSCF value 10.49 eV obtainable from (but not explicitly quoted) table 1 of Rosmus *et al* (1982). For BF, our calculations yield a vertical IP of 10.98 eV which is

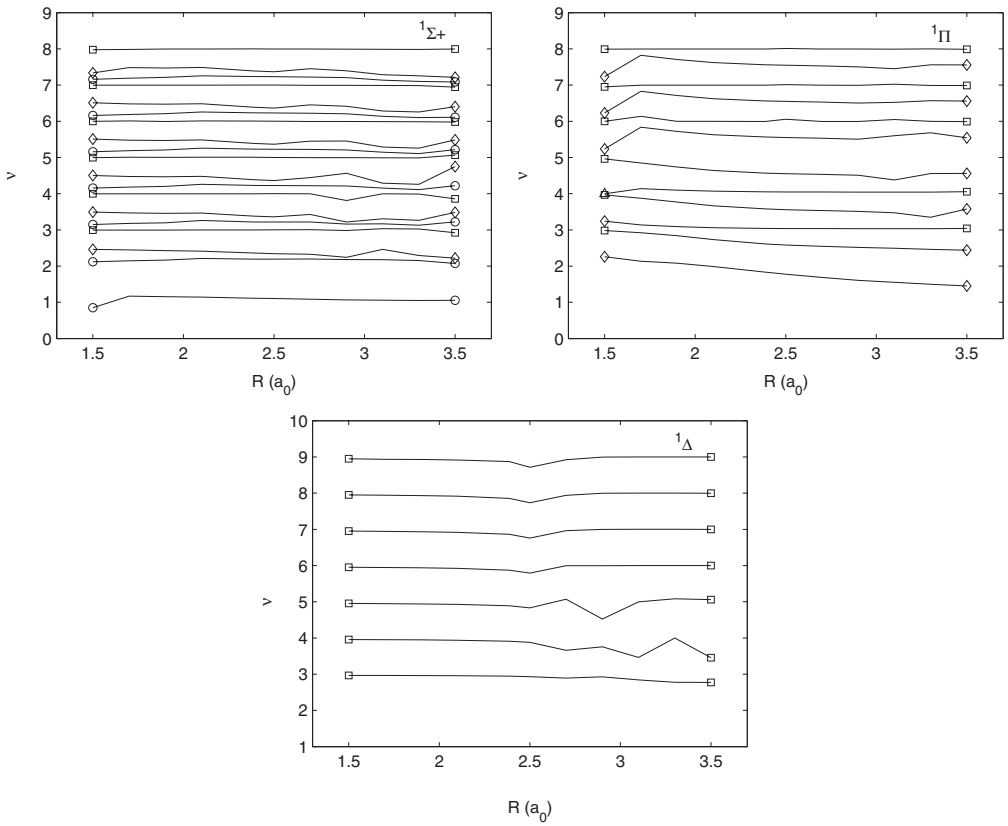


**Figure 3.** Effective quantum number $\nu$ of BF singlet bound states as a function of the bond length $R$. The $l$ character of each state is indicated by the following: ○–s, ◊–p, □–d, △–f.

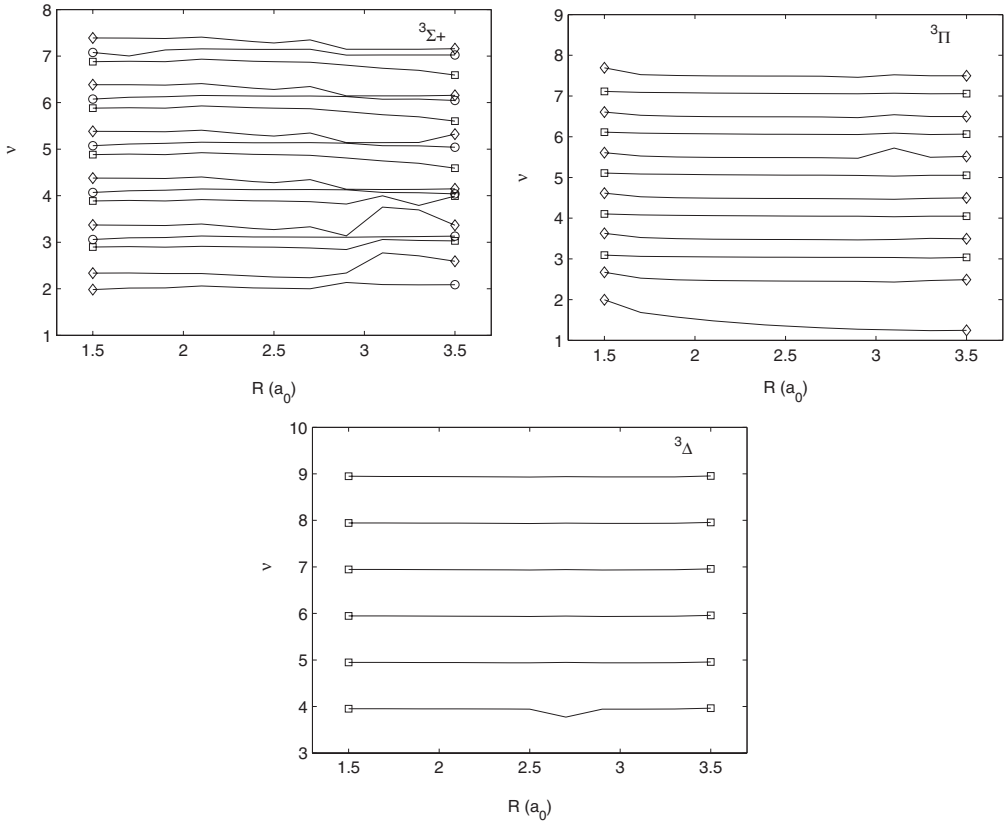


**Figure 4.** Effective quantum number $\nu$ of BF triplet bound states as a function of the bond length $R$. The $l$ character of each state is indicated by the following: ○–s, ◊–p, □–d, △–f.

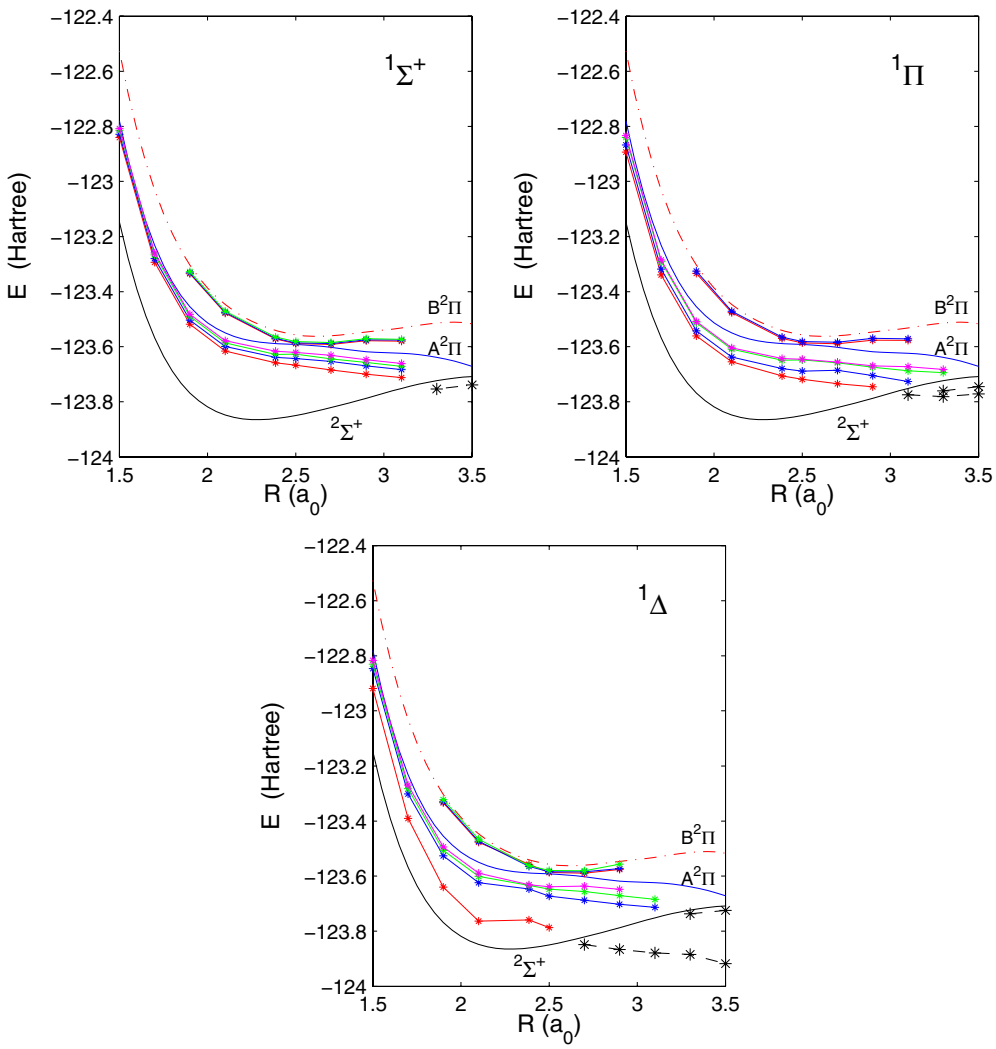


**Figure 5.** BF resonances curves of singlet symmetry with actual calculated points are indicated by stars. The symmetry of each state is indicated in the panel. Shown also are the potential energy curves of the three lowest $BF^+$ target states, the bottom most curve in black being the $X\,^2\Sigma^+$ ground state. Resonances which cross the ground state become bound.

clearly in very good agreement with experimental values of Dyke *et al* (1983) and Hildenbrand (1971).

### *3.2. Rydberg states as a function of bond length*

To obtain potential energy curves for the Rydberg states of BF, we repeated our calculations for 11 bond lengths in the range $1.5 \leqslant R \leqslant 3.5\ a_0$. The results for the lowest four curves of each symmetry are displayed in figures 1 and 2 for the singlet and triplet states respectively. All curves couple to the $X\,^2\Sigma^+$ ground state of the ion and, except for minor perturbations, are in general parallel to this.

A better and more informative method of considering the behaviour of Rydberg states as a function of geometry is to look at the quantum defects and this is done in figures 3 and 4. Generally, we find weak dependence on the B–F internuclear separation except at those positions where there are localized perturbations due to the possible presence of so-called intruder states. These states are associated with a different (excited) state of the ion that cross the ground state of the ion; at least at large internuclear separation low-lying intruder states are often valence-like in character. Intruder states result in avoided crossings which, particularly when strongly avoided, can result in wiggles appearing in the curves; such features can be seen in figures 1 and 2.

### *3.3. Resonances as a function of bond length*

In Chakrabarti and Tennyson (2009) we presented the resonance positions and widths at a single geometry. Here we present the resonances as a function of bond length for the BF states with total symmetry $^1\Sigma^+$, $^1\Pi$, $^1\Delta$ (figure 5) and $^3\Sigma^+$, $^3\Pi$ and $^3\Delta$ (figure 6). To the best of our knowledge, studies on these resonances have not been undertaken before and the data presented in this work, which can be obtained in numerical form from the first author, can be a starting point for calculation of the DR of $BF^+$. This, however, will be reported in a later work. The important resonance curves for DR are those which cross the $BF^+$ ground states and become ultimately bound. We have tried to locate these branches

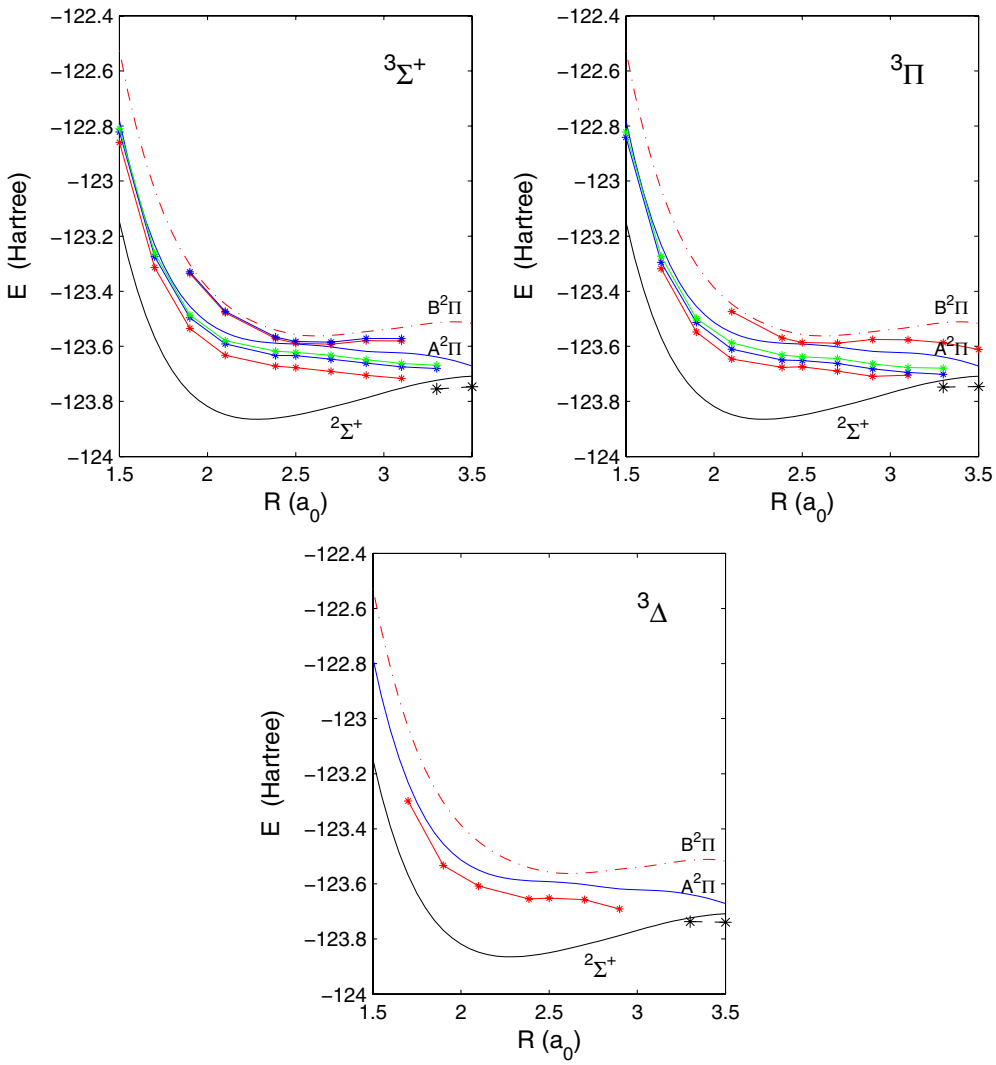


**Figure 6.** BF resonance curves of triplet symmetry with actual calculated points are indicated by stars. The symmetry of each state is indicated in the panel. Shown also are the potential energy curves of the three lowest $BF^+$ target states, the bottom most curve in black being the $X\ ^2\Sigma^+$ ground state. Resonances which cross the ground state become bound.

of potential energy curves coming from the extension of the resonances beyond the crossing point with the ion ground state curve (which are marked in figures 5 and 6 with black stars) with BOUND (Sarpal *et al* 1991), a program used to detect bound states.

## 4. Conclusion

To summarize, we have used the UK *R*-matrix molecular codes to study electron collisions with the $BF^+$ molecular ion. We obtained the bound state curves and quantum defects for the low-lying singlet and triplet states of the BF molecule. Quantum defects of the Rydberg states are presented as a function of geometry and are seen to be weekly dependent on the geometry.

The methodology employed here has been used previously to study the Rydberg state of NO (Rabadán and Tennyson 1997) and CO (Chakrabarti and Tennyson 2006). Since rather more experimental data are available for those two systems than for BF, it is possible to make some comparisons. Comparisons for the low-lying excited states considered in table 1 show errors in the vertical excitation energy in the region of 0.1–0.2 eV with the worst case, for the first excitation, being 0.6 eV. This level of accuracy is similar to that obtained previously for NO but somewhat better than that achieved for CO. While for the lower (valence) states our excitation energies are generally too high, for the higher (Rydberg) states our excitations are systematically too small. This is the combination of two effects. First, as found in previous studies, our underestimation of the effect of target polarization leads to the quantum defects being systematically underestimated. Previously this underestimate was found to be fairly uniform with the level of excitation which manifests itself as larger energy differences for the low *n* states. Second, what is really calculated in our codes is the binding energy relative to the ground state of the ion. Since our calculations underestimate the ionization potential by about 0.14 eV, this shift must also be considered. It becomes the dominant error in our excitation energies for higher states whose energies do not change much with a small shift in the quantum defect. This is why our

excitation energies for these states are too low. Whether these issues can be resolved by using the computationally much more expensive molecular *R*-matrix with the pseudostate method (Gorfinkiel and Tennyson 2004 2005) is a topic for future study.

As is the characteristics of electron collision with molecular ions, we find many series of Feshbach resonances associated with the system. The quantum defects of these resonances at equilibrium bond length were already presented in our previous work (Chakrabarti and Tennyson 2009). Here we have considered the behaviour of the resonances as a function of geometry. Particulary, we have identified those low-lying resonances which cross the target ground state and ultimately become bound. These resonances are important in DR studies of $BF^+$ which we propose to undertake later.

## Acknowledgments

KC is grateful to the French 'Conseil General de la Haute-Normandie' and to the 'Conseil National des Présidents des Universités' for a postdoctoral grant cofunded jointly by the EU under the 'People MCFR 2010' program. IFS acknowledges the scientific and financial support from the European Spatial Agency/ESTEC 21790/08/NL/HE, the International Atomic Energy Agency/CRP 'Light Element Atom, Molecule and Radical Behaviour in the Divertor and Edge Plasma Regions', the European Fusion Development Agreement and the French Research Federation for Fusion Studies, under the contract of Association between EURATOM and CEA, the French ANR-contract 'SUMOSTAI', the CNRS/INSU/'Physique et Chimie du Milieu Interstellaire' programme, the Triangle de la Physique/PEPS/'Physique théorique et ses interfaces', the CPER Haute-Normandie/CNRT/'Energie, Electronique, Matériaux', the PPF/CORIA-LOMC/'Energie-Environnement' and IEFE:Rouen & Le Havre/, contract 'Cinétique des Milieux Réactifs d'intérêt Energétique'.

## References

Bredohl H, Dubois I and Mélen F 1988 *J. Mol. Spectrosc.* **129** 145–50
Burke P G and Berrington K A 1993 *Atomic and Molecular Processes: An R-Matrix Approach* (Bristol: Institute of Physics Publishing)
Buttle P J A 1967 *Phys. Rev.* **160** 719–29
Cade P E and Huo W M 1967 *J. Chem. Phys.* **47** 614
Chakrabarti K and Tennyson J 2006 *J. Phys. B: At. Mol. Opt. Phys.* **39** 1485–97
Chakrabarti K and Tennyson J 2007 *J. Phys. B: At. Mol. Opt. Phys.* **40** 2135–45
Chakrabarti K and Tennyson J 2009 *J. Phys. B: At. Mol. Opt. Phys.* **49** 105204
Chu S I and Dalgarno A 1974 *Phys. Rev.* **10** 788–92
da Costa H F M, Simas A M, Smith V H Jr and Trsic M 1992 *Chem. Phys. Lett.* **192** 195–8
Dyke J M, Kirby C and Morris A 1983 *J. Chem. Soc. Faraday Trans.* II **79** 483–90
Ema I, García de la Vega J M, Ramírez G, López R, Fernández Rico J, Meissner H and Paldus J 2003 *J. Comput. Chem.* **24** 859
Faure A and Tennyson J 2001 *Mon. Not. R. Astron. Soc.* **325** 443–8
Gorfinkiel J D and Tennyson J 2004 *J. Phys. B: At. Mol. Opt. Phys.* **37** L343–50
Gorfinkiel J D and Tennyson J 2005 *J. Phys. B: At. Mol. Opt. Phys.* **38** 1607–22L
Giusti A 1980 *J. Phys. B: At. Mol. Phys.* **13** 3867–94
Faure A, Kokoouline V, Green C H and Tennyson J 2006 *J. Phys. B: At. Mol. Opt. Phys.* **39** 4261–73
Hildenbrand D L 1971 *Int. J. Mass Spectrom. Ion Phys.* **7** 255–60
Honingmann M, Hirsch G and Buenker R J 1993 *Chem. Phys.* **172** 59–71
Huber K P and Herzberg G 1979 *Molecular Spectra and Molecular Structure: Vol 4. Constants of Diatomic Molecules* (New York: Van Nostrand-Reinhold)
Kurtz H A and Jordan K D 1981 *Chem. Phys. Lett.* **81** 104–9
Lim A J, Rabadán I and Tennyson J 1999 *Mon. Not. R. Astron. Soc.* **306** 473–8
Mérawa M, Bégué D, Rérat M and Pouchan C 1997 *Chem. Phys. Lett.* **280** 203–11
Morgan L A 1984 *Comput. Phys. Commun.* **31** 419
Morgan L A, Tennyson J and Gillan C J 1998 *Comput. Phys. Commun.* **114** 120–8
Noble C J and Nesbet R K 1984 *Comput. Phys. Commun.* **33** 399–411
Rabadán I and Tennyson J 1996 *J. Phys. B: At. Mol. Opt. Phys.* **29** 3747–61
Rabadán I and Tennyson J 1997 *J. Phys. B: At. Mol. Opt. Phys.* **3** 1975–88
Rabadán I and Tennyson J 1998 *Comput. Phys. Commun.* **114** 129–41
Rosmus P, Werner H J and Grim M 1982 *Chem. Phys. Lett.* **92** 250–6
Sarpal B K, Branchett S E, Tennyson J and Morgan L A 1991 *J. Phys. B: At. Mol. Opt. Phys.* **24** 3685–99
Schneider F and Gianturco F A 1988 *J. Phys. B: At. Mol. Opt. Phys.* **21** 329
Schneider I F, Rabadán I, Carata L, Anderson L H, Suzor-Weiner A and Tennyson J 2000 *J. Phys. B: At. Mol. Opt. Phys.* **33** 4849–61
Tennyson J 1996a *J. Phys. B: At. Mol. Opt. Phys.* **29** 1817–28
Tennyson J 1996b *J. Phys. B: At. Mol. Opt. Phys.* **29** 6185–201
Tennyson J 2010 *Phys. Rep.* **491** 29–76
Tennyson J, Burke P G and Berrington K A 1987 *Comput. Phys. Commun.* **47** 207–12
Tennyson J and Morgan L A 1999 *Phil. Trans. R. Soc.* A **357** 1161–73
Tennyson J and Noble C J 1984 *Comput. Phys. Commun.* **33** 421–4
Zhang R, Franz J, Baluja K L and Tennyson J 2011 *J. Phys. B: At. Mol. Opt. Phys.* **44** 035203